Article

Molecular Dynamics and Chain Length of Edible Oil by Low-Field Nuclear Magnetic Resonance

Zijian Jia [1,*] and Can Liang [2]

[1] University of Shanghai for Science and Technology, 516 Jungong Rd.Shanghai 200093, P.R.China.
[2] Changzhou Institute of Technology, 666, Liaohe Road, Changzhou, 213032, P.R.China.
* Correspondence: jiazijian1989@usst.edu.cn;

Abstract: Nuclear magnetic resonance (NMR) techniques are widely used to identify pure substances and probe protein dynamics. Edible oil is a complex mixture composed of hydrocarbons, which have a wide range of molecular size distribution. In this research, low field NMR (LF-NMR) relaxation characteristic data of various sample oils were analyzed. We also suggest a new method for prediction size of edible oil molecules using LF-NMR relaxation time distributions. According to the relative molecular mass, carbon chain length, transverse relaxation time of different sample oils, combined with oil viscosity and other factors, the relationship between carbon chain length and transverse relaxation time rate was analyzed. Various oils and fats in the mixed fluid are displayed, reflecting the composition information of different oils. To study the correlation between the rotation correlation time and molecular information of oil molecules. The molecular composition of the resulting fluid determines its properties, such as viscosity and phase behavior. The results show that low-field NMR can obtain information on the composition, macromolecular aggregation, and molecular dynamics of complex fluids. Measurements of grease in the free fluid state show that the relaxation time can reflect the intrinsic properties of the fluid. It is shown that the composition characteristics and states of complex fluids can be measured by low-field nuclear magnetic resonance.

Keywords: Low-field NMR; Two-dimensional nuclear magnetic resonance; Edible oil; Chain length; rotation correlation time;

1. Introduction

Nuclear magnetic resonance (NMR) is a powerful tool for qualitative and quantitative analysis of organic and inorganic substances. Low-field nuclear magnetic resonance (LF-NMR) technology is a new technical means to observe and analyze the physical parameters of samples gradually developed in recent years. At the same time, it symbolizes that the research direction of medical detection technology and complex high-end molecular and chemical materials structure is developing towards a wider range of industrial and agricultural fields. NMR technology can not only observe and analyze the information inside the material without damaging the sample, but also has the advantages of fast, accurate, non-invasive, no environmental pollution, no radiation and so on. High-field NMR equipment has high sensitivity, high resolution and high signal-to-noise ratio, but it has high requirements on sample uniformity. Liquid needs to be deionized and solid needs to be powdered. In addition, the instrument is expensive, and the cost of subsequent maintenance equipment is extremely high. LF-NMR devices, however, use permanent magnets, making them small and cheap. Ideal for online process inspection, industrial quality control and quality inspection. Compared with high-field NMR, LF-NMR is low in both capital and time cost.

In the food field, the mixed porous medium composed of water and oil exists in most food materials, and the relaxation rate of samples is affected by the pore size. Therefore, the measurement of pore distribution and the distinction between oil and water can be detected and analyzed by LF-NMR. This can also play an important role in the quality

Preprints (www.preprints.org) | NOT PEER-REVIEWED | Posted: 14 November 2022 doi:10.20944/preprints202211.0253.v1

control of food safety, such as edible oil [1-4], yellow croaker [5], prawn [6, 7] and etc. The transverse relaxation decay curve of LF-NMR can not only monitor the quality of frying oil based on the prediction of physicochemical indexes such as viscosity, acid value, and carbonyl value[8], but also elucidate the correlation between the biophysical state of intrinsic water and structural properties in dried fermented meat products[9]. What' s more, analysis of transverse relaxation decay curves also plays an important role in food quality control. It has been widely used in analytical detection of food products like edible oil incorporation artifact detection[10], soybean variety discrimination[11], and meat quality analysis[12].

1H NMR spectroscopy has been widely used in the analysis of oil which has been applied to the determination of vegetable oil bio sources[13] and quantification of vegetable oil fatty acid profiles[14]. Techniques based on 1H NMR spectroscopy have been intensively developed aiming to characterize the bio oil composition, monitor the bio oil production process, and evaluate the bio oil concentration in bio oils and their mixtures[15]. The determination of carbon chain length is very important for liquid fuels because it is one of the key parameters determining their quality and performance. And it also strongly influences other quality parameters like the viscosity of liquid fuels, higher thermal values and hexadecane values. The correlation of experimentally obtained T_2 relaxation times with viscosity and other physical parameters of different kinds of vegetable oil oils and oils is empirically described in most studies. NMR relaxation is used to explain the T_2 dependence on the viscosity of alkanes, considering the shape of spherical molecules[16].

In this work, we applied low field NMR to study the molecular structures of fatty acids and glycerides. According to the correlation between relaxation rates and carbon chain lengths of fatty acid mixtures, it suggests that low field NMR has the potential to serve as a method for rapidly measuring the properties of the oily moieties.

2. Materials and Methods

Molecular motion determines the relaxation time and information about molecular components which is available. The spin dynamics of a fluid are characterized by the longitudinal relaxation time T_1, transverse relaxation time T_2 of the spin system, and the diffusion coefficient D of the whole molecule. Among relatively complex fluid mixtures, the small molecules diffuse more rapidly than the large one due to molecular volume. Thus, the diffusion coefficient of a particular hydrocarbon molecule is related to its size or chain length and the overall fluid environment can affect molecular diffusion. For any relatively complex compound molecule, the relaxation time is determined by intramolecular nuclear dipole interactions, which are influenced by molecular motions. The longitudinal relaxation time T_1 is related to the overall molecular rotational tumbling in solution because the frequency of tumbling must be matched with the frequency of spin transitions required for spin lattice energy transfer. Transverse relaxation explains that the rapid phase dispersion of XY magnetization at a rate of $1/T_2$ by an intramolecular dynamic process in the XY plane. At this time the longitudinal relaxation time T_1 is longer than or equal to the transverse relaxation time T_2. The rotational correlation time represents that it took time T for the particle to rotate one arc in solution. It is determined by the size and shape of the particles. The rate of molecular trigger was estimated from the Stokes Einstein equation(Eq.)[17-18]:

$$\frac{1}{\tau_c} = \frac{3kT}{4\pi\eta r_g^3} \quad (1)$$

According to the formula, $1/\tau_c$ is the trigger rate, r_g is the radius of gyration, η is the viscosity of the solvent, k is Boltzmann constant and T is Kelvin temperature. The theoretical model, which is a model between the Brownian motion of the molecule and the NMR relaxation time, which was built on the basis of bloembergen's theory. The relaxation rate of the protons within a sample as a function of the rotational correlation time of the molecule τ_c is shown below:

Preprints (www.preprints.org) | NOT PEER-REVIEWED | Posted: 14 November 2022 doi:10.20944/preprints202211.0253.v1

$$\frac{1}{T_1} = \frac{3}{10}\left(\frac{\mu_0}{2\pi}\right)^2 \frac{\gamma^4 \hbar^2}{l^6}\left[\frac{\tau_c}{1+\omega_0^2\tau_c^2} + \frac{4\tau_c}{1+4\omega_0^2\tau_c^2}\right] \quad (2)$$

$$\frac{1}{T_2} = \frac{3}{20}\left(\frac{\mu_0}{2\pi}\right)^2 \frac{\gamma^4 \hbar^2}{l^6}\left[3\tau_c + \frac{5\tau_c}{1+\omega_0^2\tau_c^2} + \frac{2\tau_c}{1+4\omega_0^2\tau_c^2}\right] \quad (3)$$

In these formulas ,ℏ is the rationalized Planck constant that Planck constant is divided by 2 π. γ Is the permeability as the ratio of magnetic induction strength B to magnetic field strength h in a magnetic medium. μ_0 is the permeability over free space, where f is the 1H Larmor precession frequency which means ω_0=2πf. l is the distance between adjacent two hydrogen nuclei which are located on the same compound molecule.

According to Eq. (3) and (4), the downfield NMR relaxation times T_1 relaxation times and T_2 relaxation times are different if the oil contains macromolecular structures. For rapidly moving molecules, both T_1 relaxation times and T_2 relaxation times decrease with increasing t. For molecules in slow motion, T_2 relaxation times decrease with increasing τ_c, T_1 relaxation times increase with increasing τ_c, and T_1 relaxation times are longer than T_2 relaxation times. The size of the molecular aggregates and macromolecules is larger than isolated molecules. The reason why T_1 relaxation times is longer than T_2 relaxation times may be caused by the low trigger rotation rates of these structures. Whether relaxation time T_1 or relaxation time T_2, it is determined by the rotational correlation time. Thus, NMR relaxation reflects molecular motion: small molecules diffuse more rapidly than large molecules. Thereby it indicates that all spins on the same molecule in similar solvents have comparable relaxation times.

$$\frac{T_1}{T_2} = \frac{1}{2}\frac{5(1+\omega_0^2\tau_c^2)^{-1} + 2(1+4\omega_0^2\tau_c^2)^{-1} + 3}{(1+\omega_0^2\tau_c^2)^{-1} + 4(1+4\omega_0^2\tau_c^2)^{-1}} \quad (4)$$

The viscosity of a fluid sample is jointly determined by all the components in that fluid. It can be analyzed according to EQS (2) and (3) that the longitudinal relaxation time is equal to the transverse relaxation time at low magnetic field strength for a fluid of lower viscosity. If the T_1 relaxation time is not equal to the T_2 relaxation time, this indicates the presence of slower motions compared to the molecular size related motions, which generally occurs in the presence of aggregated polymeric molecules with larger size aggregated in the fluid. Figure1 demonstrates that molecular motion is accelerated (for the lamore frequency of atoms) when ω_0 τ_c<1, while for a given one, both T_1 relaxation times and T_2 relaxation times decrease as τ_c increases. But when the rate of molecular motion is gradually slowed down, the T_2 relaxation time will continue to decrease while the T_1 relaxation time will start to increase. This result most likely coused by supramolecular structures or intramolecular aggregation.

Preprints (www.preprints.org) | NOT PEER-REVIEWED | Posted: 14 November 2022 doi:10.20944/preprints202211.0253.v1

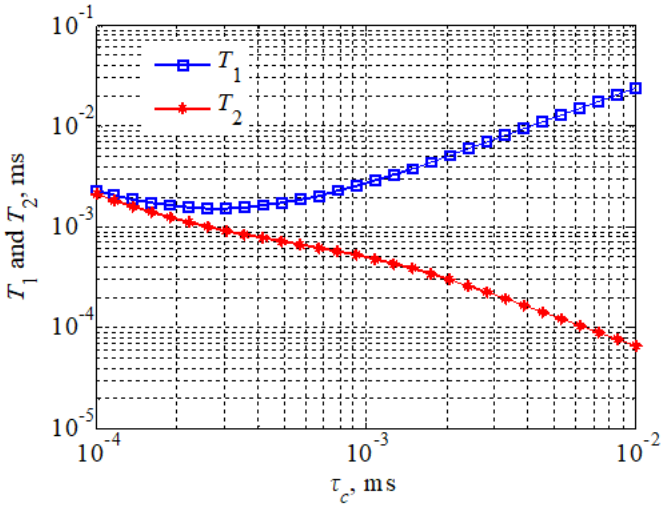

Figure 1. Theoretical plots of T_1, T_2 relaxation times versus Lamore frequency and correlation times.

3. Experiment

The samples of oils used in this experiments were varied vegetable oils which are mainly composed of glycerides and fatty acids. Oil and oil samples kept at a constant temperature were loaded into the test tubes and labeled. It should be capped and sealed in order to avoid volatilization of the light hydrocarbon components during NMR relaxometry, which ensured accurate, effective and error free relaxation time measurement data results. Samples with different average carbon chain lengths were prepared as different mixtures of several common vegetable oil oils and fats. The oils and fats in this study were selected based on their properties and melting point should be below 25°C for measurement at room temperature. Their properties (molecular weight, state and molecular carbon chain length) are given in table1.

NMR spectra of oils are characterized by overlapping signals of a wide variety of fatty acids, which come from among different triglyceride combinations. Calculate the transverse relaxation time T_2 by using the hard pulse CPMG sequence, and set the half echo time and number of echoes. In this experiment, the number of repeated scans can generally be set as 16 times because the signal intensity of oil is relatively strong enough to the moisture signal. The sampling frequency setting is set to around 250kHz in order to get more effective signals in grease. Its parameters are shown below : Repetitive sampling latency TR is about 1 s; The echo time TE is taken to be 6 ms; The number of pulses in the 180 ° sequence is taken to be 600; The echo number was taken around 1000; The main value SF of the RF signal frequency is taken to be 23 MHz; Measurements for all experiments are performed at room temperature (25 ° C).

Preprints (www.preprints.org) | NOT PEER-REVIEWED | Posted: 14 November 2022 doi:10.20944/preprints202211.0253.v1

Table 1. Oils and fats for sample preparation.

Formula	Name	Ar	Chain length	Status	Purity
$C_3H_8O_3$	glycerol	92	3	Liquid viscous	98%
$C_4H_8O_3$	Glyceraldehyde	104	4	Liguid	98%
$C_6H_{14}O_5$	Diglycerol	166	6	Liquid viscous	80%
$C_6H_{12}O_3$	Ketal glycerol	132	6	Liquid	>=95%
$C_7H_{12}CLN_3O_2$	Syringolin	205.5	7	Liquid	AR,>=80%
$C_{10}H_{16}$	Turpentine	136	10	Liquid	AR
$C_{10}H_{18}O$	Terpineol	154	10	Liquid	AR
$C_{12}H_{20}O_6$	Glyceryl tripropanoate	260	12	Liquid	>=95%
$C_{12}H_{20}O_2$	Turpentine acetate	196	12	Liquid	>=97%
$C_{15}H_{26}O_6$	Tributyrin	302	15	Liquid	98%
$C_{18}H_{34}O_2$	Oleic acid	282	18	Liquid	AR
$C_{18}H_{37}N$	Oleylamine	267	18	Solid	80-90%
$C_{18}H_{36}O$	Oleyl alcohol	268	18	Liquid	80-85%
$C_{19}H_{36}O_2$	Methyl oleate	296	19	Liquid	99%
$C_{20}H_{36}O_2$	Linoleic acid ethyl ester	308	20	Liquid	>=97%
$C_{20}H_{38}O_2$	Ethyl oleate	310	20	Liquid	75%
$C_{21}H_{20}O_6$	Ginger butter	368	21	Liquid	>=98%
$C_{21}H_{42}O_4$	Propylene Glycol Ole ate	358	21	Semisolid	95%
$C_{22}H_{42}O_2$	Butyl oleate	338	22	Liquid	AR
$C_{24}H_{38}O_4$	Perilla leaf oil	390	24	Liquid	>=55%
$C_{24}H_{47}NO_4$	Triethanolamine oleic acid soap	413	24	Liquid	92%
$C_{27}H_{50}O_6$	Trioctanoin	470	27	Liquid	>=99%
$C_{30}H_{62}O_{21}$	Decaprenylglycerol	758	30	Solid	98%
$C_{38}H_{46}N_2O_8$	Cocamine	658	38	Solid	98%
$C_{39}H_{76}O_5$	Distearate	624	39	Solid	97%
$C_{39}H_{74}O_6$	Glycerol trilaurate	638	39	Solid	98%
$C_{45}H_{76}O_2$	Linoleate cholesteryl es-ter	648	45	Solid	95%
$C_{51}H_{98}O_6$	Tripalmitin	806	51	Solid	98%
$C_{57}H_{110}O_6$	Tristearin	890	57	Solid	98%

4. Data analysis

Because the viscosity of some oils is different, the longer the carbon chain length of the oil is, the higher the saturation degree of the oil is, and the greater the viscosity of the oil is. On the contrary, the shorter the carbon chain length of the oil, the lower the saturation degree of the oil, and the lower the viscosity of the oil. Fig.2 and Fig.3 shows the measured results of T_1-T_2 distribution of 8 different oils. The first type of oi l is characterized by high saturation, high viscosity, and shorter relaxation time than other oils, which is only within 10ms, such as glycerin, diglycerin, etc; The second type is resin. The T_1 relaxation time of resin containing grease is longer than T_2 relaxation time. The interaction with other oil molecules slows down the rotation of maltene molecules when they are close to each other. This reaction results in a shorter relaxation time, such as terpineol. These results indicate that the distribution of T_1-T_2 is related to the physical properties and chemical composition of oils. Therefore, the T_1-T_2 distribution shape can be used to identify different grease properties as shown in Fig 2 and Fig 3.

Figure 2. This is a figure. Schemes follow another format. If there are multiple panels, they should be listed as: (**a**) Description of what is contained in the first panel; (**b**) Description of what is contained in the second panel. Figures should be placed in the main text near to the first time they are cited.

Preprints (www.preprints.org) | NOT PEER-REVIEWED | Posted: 14 November 2022 doi:10.20944/preprints202211.0253.v1

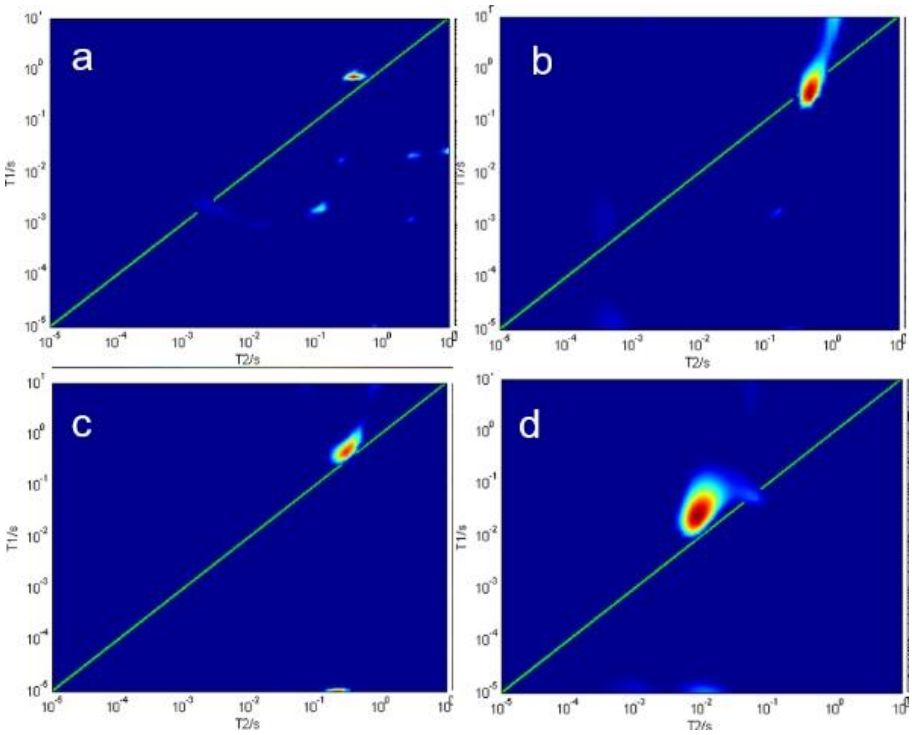

Figure 2. T_1-T_2 distribution of 4 oil samples at room temperature (25 ℃). In each chart, the green line is T_1=T_2 line. (a) $C_6H_{12}O_3$, (b) $C_7H_{12}CLN_3O_2$, (c) $C_{12}H_{20}O_2$, (d) $C_{24}H_{47}NO_4$.

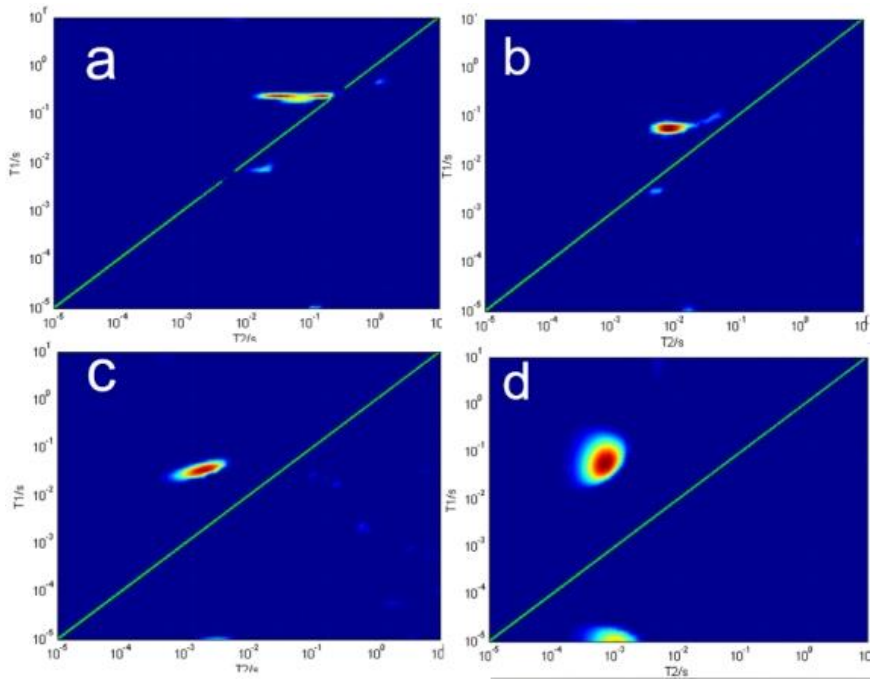

Figure 3. T_1-T_2 distribution of 4 oil samples at room temperature (25 ℃). In each chart, the green line is T_1=T_2 line. (a) $C_{21}H_{42}O_4$, (b) $C_{24}H_{47}NO_4$, (c) $C_{30}H_{62}O_{21}$, (d) $C_{57}H_{98}O_{12}$.

As the oil is below the appearance temperature for solidification, crystals emerge and the sample becomes solid (Fig 3). The gel contains a rigid network that stops the oil from flowing. The network can consist of a fraction of the weight of the sample; At the molecular level, most oil molecules remain fluid. T_2 is unchanged and T1 is increased, indicating that the rotation of most oil molecules is not affected by the formation of rigid networks. Note that in this case, oil viscosity cannot be predicted from relaxation measurements alone.

Preprints (www.preprints.org) | NOT PEER-REVIEWED | Posted: 14 November 2022 doi:10.20944/preprints202211.0253.v1

The theoretical relationship between the distribution and T_1, T_2, T_1/T_2 can be obtained from Eq. (4). Combined with the measured T_1/T_2 distribution and this theoretical relationship. The results were analyzed to reveal the movement differences of each type and size of molecules in the fluid. Molecular dynamics reflects fluid. The distribution of rotation correlation time also reflects the rotation correlation time of all molecules, which can be used to analyze the molecular dynamics of complex fluids.

Therefore, affected by the viscosity and molecular structure of different vegetable oils, some oils with similar viscosity and molecular structure are selected for data analysis and processing (Table2).

Table 2. Experimental values of carbon chain length and spin-spin relaxation rate of oils.

Formula	Name	Chain Length	Status	T_2 (s)	R_2 (s^{-1})
$C_4H_8O_3$	Glycerol formal	4	liquid	4.51	0.221729
$C_6H_{12}O_3$	Solketal	6	liquid	3.62	0.276243
$C_7H_{12}CLN_3O_2$	Clove Oil	7	liquid	5.2	0.192308
$C_{12}H_{20}O_6$	Tripropionin	12	liquid	3.62	0.276243
$C_{12}H_{20}O_2$	Terpinyl Acetate	12	liquid	3.25	0.307692
$C_{15}H_{26}O_6$	Tributyrin	15	liquid	3.25	0.307692
$C_{18}H_{37}N$	Oleylamine	18	Semisolid	4.04	0.247525
$C_{19}H_{36}O_2$	methyl oleate	19	liquid	5.2	0.192308
$C_{20}H_{36}O_2$	ethyl linoleate	20	liquid	5.03	0.198807
$C_{20}H_{38}O_2$	Ethyl Oleate	20	liquid	6.26	0.159744
$C_{21}H_{20}O_6$	Curcuma oil	21	liquid	9.7	0.103093

In the experiment, the transverse relaxation time rate R_2 depends on the composition of different oil molecules in the sample. The Bloombergen-Purcell-Pound (BPP) method is usually used to describe the spin spin NMR relaxation in liquids. According to the BPP theory, the spin -spin relaxation time T_2 or the relaxation rate R_2 ($R_2=1/T_2$) depends on the molecular rotation rate expressed by the rotation correlation timeτ_c, which is a characteristic parameter of the molecular rotation rate. The liquid sample$\omega_0\ \tau_c \ll 1$ (the resonance frequency of the nuclear magnetic resonance device) and R2 increase linearly with the increase of the relevant time, as shown below:

$$R_2 = 10M_2\tau_c \tag{5}$$

In the equation, M_2 is the value of the second order matrix, which is determined by the intensity of dipole-dipole interaction between adjacent atomic nuclei. The rotation correlation time in the BPP equation can be described by the Stokes-Einstein -Debye equation:

$$\tau_c = \frac{C_r \eta V}{K_B T} \tag{6}$$

Where, V is the effective volume of the molecule, η is the viscosity,T is the Kelvin temperature, K_B is the Boltzmann constant and is determined by experiments, and C_r is the fitting parameter. Stokes-Einstein-Debye equation is usually used for homogeneous fluid in the modified form, and its molecules are described as spheres with hydrodynamics or Stokes radius, rather than molecules.

The rotation related motion contributes the most to the NMR relaxation spectrum, while the frequency range of the translation motion contributes less to the NMR relaxation proton spectrum. The NMR relaxation does not observe that the vibration is due to its high amplitude frequency. The rotation correlation time of different molecular motions is a time parameter in a specific correlation function. Complex modeling is required to describe them separately. On the other hand, the rotational correlation time of molecules can be calculated by the known corresponding diffusion coefficient, which is described by Stokes-Einstein equation:

Preprints (www.preprints.org) | NOT PEER-REVIEWED | Posted: 14 November 2022 doi:10.20944/preprints202211.0253.v1

$$D_r = \frac{K_B T}{8\pi\eta R^3} \quad (7)$$

Where, D_r is the rotational diffusion coefficient, K_B is the Boltzmann constant, T is the temperature, η is the viscosity and R is the Stokes molecular radius. When describing the rotational motion of molecules, it is easy to think that molecules have spherical shape of hydrodynamic radius. Considering that the effective volume of the molecule is equal to:

$$V = \frac{4\pi R^3}{3} \quad (8)$$

The combination of Eq. (5) (6) and (7) gives the following results:

$$\tau_c \sim \frac{1}{D_r} \quad (9)$$

Therefore, it is clear that the rotation correlation time depends on the corresponding diffusion coefficient (Eq.8). Eq. (8) is a widely used ratio for calculating the NMR relaxation correlation time, because the rotational molecular motion is the main contributor to NMR relaxation. In general, molecules with different shapes can be characterized by hydrodynamic radii. Therefore, Eq. (8) may be applicable to both unbranched rod molecules (mainly in liquid biofuels) and different types of paraffins and aromatics in petroleum fuels. In order to correlate the rotational diffusion coefficient with the molecular weight, known ratios can be used to describe the self diffusion and self behavior of the untwisted polymer chain. For elongated, unbranched molecules, there is a direct dependency between these two parameters:

$$D_{self} \sim M_w^{-\alpha}, \quad M_w < M_{wc} \quad (10)$$

Where M_{wc} is the entanglement coupling molecular weight, α is the coefficient, equal to 1. Combining Eq. (6), (8) and (9), we can clearly see the linear relationship between and molecular weight.

$$R_2 \sim M_w \quad (11)$$

It is easy to assume that in the case of unbranched hydrocarbons with similar chemical organization, the molecular weight is proportional to the molecular size, which can be evaluated by CL. Dependent on the dependence of R_2 on the molecular weight M_w (Eq.10), assume that R_2 is linearly dependent on CL:

$$R_2 \sim \mathrm{CL} \quad (12)$$

The decay of CPMG pulse echo sequence of all oil samples was measured, and then the spin spin relaxation rate R_2 was determined by single exponential function fitting. Results of R_2 values are collected in Table 2. The carbon chain length CL is plotted as a function of the relaxation rate in Fig. 4, showing a linear relationship. By applying a linear fit to the dataset, the model can be calculated as follows:

$$\mathrm{CL}_{NMR} = a R_2 + b \quad (13)$$

Where a = - 43.713 s， b = 23.869.

Preprints (www.preprints.org) | NOT PEER-REVIEWED | Posted: 14 November 2022 doi:10.20944/preprints202211.0253.v1

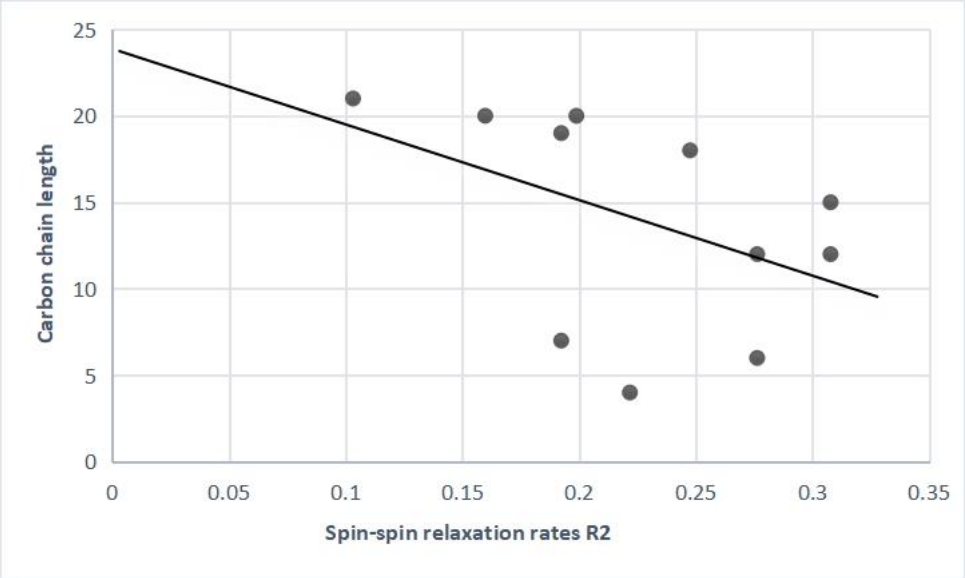

Figure 4. The carbon chain length CL is plotted as a function of the relaxation rate R_2. Solid line is fitted by linear model.

In this study, the carbon chain length of oil mixture has been determined by LF-NMR, which shows a good consistency with the known. Grease is selected according to their properties, so it is lower than room temperature. However, in addition to the main components, specific profiles can also contain oils with higher carbon chain lengths (more than 20). Therefore, the carbon chain length of general vegetable oils is generally longer than that of CL used in this study. From Eq.13 and our experimental results, it can be seen that the relaxation rate of oil molecules has a linear relationship with the length of carbon chain. It is clear that this relationship applies to longer molecules.

5. Conclusions

We use NMR relaxation to measure vegetable oil, collect and analyze NMR signals of more than 20 different kinds of vegetable oil samples, obtain the transverse relaxation time and its rate of oil samples, and determine the possible interaction of these molecules by inferring and analyzing the relationship between the length of oil carbon chain and the transverse relaxation time rate through the study of oil composition and molecular structure. The rotation correlation time is used to characterize the rotation correlation time of oil molecules. The rotation correlation time depends on the molecular size, dynamics and solvent properties. The influence of oil viscosity on transverse relaxation time and longitudinal relaxation time is obtained. The smaller the viscosity is, the greater the T_2 relaxation time is, and the higher the oil viscosity will be, leading to the smaller T_2 relaxation time. The same is true for T_1 relaxation time. The factors that affect the viscosity of oil are the common influence of glycerides and fatty acids in various oil compositions. The length of fatty acid chain in glycerides and the saturation degree of fatty acid chain length are determined. The longer the carbon chain of fatty acids is, the higher the saturation degree of oil will be, which will make the viscosity of oil more viscous. On the contrary, the shorter the carbon chain length of the oil, the lower the saturation degree of the oil, and the lower the viscosity of the oil. Therefore, NMR relaxation reflects molecular motion. Small molecules diffuse farther and rotate faster than large molecules, indicating that all spins on the same molecule in similar solvents have considerable relaxation time.

The results of this study show that the rotation related time distribution is directly related to the molecular size distribution and molecular dynamics in oil solution. The rotation correlation time of oil also reflects the interaction between molecules and the viscosity of oil solution. The measurement results of oil in free fluid state show that the relaxation reflect the inherent properties of the fluid.

Author Contributions: Conceptualization, Zijian Jia. and Can Liang.; data curation, Zijian Jia.; writing—original draft preparation, Zijian Jia.; writing—review and editing, Can Liang. All authors have read and agreed to the published version of the manuscript.

Acknowledgments: This research was supported by the National Natural Science Foundation of China (NSFC China 81773482, 31201365); the Key Scientific and Technological Projects of Science and Technology Commission of Shanghai Municipality (18142201200); the Development of Major Scientific Instruments and Equipment of the State (2013YQ17046303); and the Shanghai Key Laboratory of Molecular Imaging (18DZ2260400).

References

1. Zhao T T, Wang X, Hai-Yan L U, et al. The Quality Assessment of Edible Oils and Fats by LF-NMR Coupled with PCA [J]. Modern Food Science & Technology, 2014, 30(9): 179-185.
2. Zhu W, Wang X, Chen L. Rapid detection of peanut oil adulteration using low-field nuclear magnetic resonance and chemometrics [J]. Food chemistry, 2017, 216: 268-274.
3. Santos P M, Kock F V C, Santos M S, et al. Non-invasive detection of adulterated olive oil in full bottles using time-domain NMR relaxometry [J]. Journal of the Brazilian Chemical Society, 2017, 28(2): 385-390.
4. Wu J, Li Y, Gao X. Simultaneous determination of oil and water in soybean by LF-NMR relaxometry and chemometrics [J]. Chemical Research in Chinese Universities, 2016, 32(5): 731-735.
5. Zang X, Lin Z, Zhang T, et al. Non-destructive measurement of water and fat contents, water dynamics during drying and adulteration detection of intact small yellow croaker by low field NMR [J]. Journal of Food Measurement and Characterization, 2017, 11(4): 1550-1558.
6. Li M, Li B, Zhang W. Rapid and non-invasive detection and imaging of the hydrocolloid-injected prawns with low-field NMR and MRI [J]. Food chemistry, 2018, 242: 16-21.
7. Wang H, Wang R, Song Y, et al. A fast and non-destructive LF-NMR and MRI method to discriminate adulterated shrimp [J]. Journal of Food Measurement and Characterization, 2018, 12(2): 1340-1349.
8. Sun Y, Zhang M, Fan D. Effect of ultrasonic on deterioration of oil in microwave vacuum frying and prediction of frying oil quality based on low field nuclear magnetic resonance (LF-NMR) [J]. Ultrasonics sonochemistry, 2019, 51: 77-89.
9. García A B G, Rodríguez M I C, de Ávila Hidalgo M D R, et al. Water mobility and distribution during dry-fermented sausages "Spanish type" manufacturing and its relationship with physicochemical and textural properties: a low-field NMR study [J]. European Food Research and Technology, 2017, 243(3): 455-466.
10. Wang X, Wang G, Hou X, et al. A Rapid Screening Approach for Authentication of Olive Oil and Classification of Binary Blends of Olive Oils Using Low-Field Nuclear Magnetic Resonance Spectra and Support Vector Machine [J]. Food Analytical Methods, 2020, 13(10): 1894-1905.
11. Jiang Chao, Han Jianzhong. Rapid identification of rice varieties based on low-field NMR technology [J]. Science and Technology of Food Industry, 2012, 33(6): 64-66.
12. Gai S, Zhang Z, Zou Y, et al. Rapid and non-destructive detection of water-injected pork using low-field nuclear magnetic resonance (LF-NMR) and magnetic resonance imaging (MRI) [J]. International Journal of Food Engineering, 2019, 15(8).
13. Fauhl C, Reniero F, Guillou C. 1H NMR as a tool for the analysis of mixtures of virgin olive oil with oils of different botanical origin[J]. Magnetic Resonance in Chemistry, 2000, 38(6): 436-443.
14. Knothe G, Kenar J A. Determination of the fatty acid profile by 1H-NMR spectroscopy[J]. European Journal of Lipid Science and Technology, 2004, 106(2): 88-96.
15. Monteiro M R, Kugelmeier C L, Pinheiro R S, et al. Glycerol from biodiesel production: Technological paths for sustainability[J]. Renewable and Sustainable Energy Reviews, 2018, 88: 109-122.
16. Hürlimann M D, Freed D E, Zielinski L J, et al. Hydrocarbon composition from NMR diffusion and relaxation data[J]. Petrophysics-The SPWLA Journal of Formation Evaluation and Reservoir Description, 2009, 50(02).
17. Einstein A, On the movement of small particles suspended in stationary liquids required by the molecular-kinetic theory of heat[J], Annalen der Physik, 17(1905)549-560
18. Bloembergen N, Purcell E M, Pound R V, Relaxation effects in nuclear magnetic resonance absorption[J], Physical Review, 73(1948)679-746.